Energy transfer and device performance in phosphorescent dye doped polymer light emitting diodes

Yong-Young Noh, Chang-Lyoul Lee, and Jang-Joo Kim[a)]
Department of Materials Science and Engineering, Kwangju Institute of Science and Technology, 1 Oryong-Dong, Buk-Gu, Kwangju 500-712, South Korea

Kiyoshi Yase
Photonics Research Institute, National Institute of Advanced Industrial Science and Technology (AIST), 1-1-1 Higashi, Tsukuba, Ibaraki 305-8565, Japan

(Received 19 April 2002; accepted 12 November 2002)

Singlet and triplet–triplet energy transfer in phosphorescent dye doped polymer light emitting devices were investigated. Poly(*N*-vinylcarbazol) and poly[9,9′-di-*n*-hexyl-2,7-fluorene-alt-1,4-(2,5-di-*n*-hexyloxy)phenylene] (PFHP) were selected as the host polymer for the phosphorescent dopants *fac*-tris(2-phenylpyridine) iridium(III) [$Ir(ppy)_3$] and 2,3,7,8,12,13,17,18-octaethyl-21H,23H-porphyrin platinum(II) (PtOEP) because of their high triplet energy levels and long phosphorescence lifetimes. In case of PVK film, efficient triplet energy transfers to both PtOEP and $Ir(ppy)_3$ were observed. In contrast, the triplet energy transfer did not occur or was very weak from PFHP to both PtOEP and $Ir(ppy)_3$ although usual requirements for triplet energy transfer were satisfied. Furthermore, the singlet–singlet energy transfer did not take place from PFHP to $Ir(ppy)_3$ in doped films even though the Förster radius is more than 30 Å. However, the blended film of $Ir(ppy)_3$ with PFHP and PMMA showed the green emission from $Ir(ppy)_3$ via singlet energy transfer. In addition, the solution of PFHP and $Ir(ppy)_3$ (8 wt. %) in *p*-xylene also showed green emission. The blocking of the energy transfers in the phosphorescent dye doped PFHP films is found to be originated from the formation of aggregates which is evident from the microscopic images taken by transmission electron microscope, atomic force microscope, and fluorescence microscope. The formation of aggregates prevents dopant molecules from being in close proximity with host molecules thereby inhibiting energy transfer processes. The phase separation deteriorates the device performance also. Therefore, the chemical compatibility of a dopant with a host polymer as well as conventional requirements for energy transfers must be significantly considered to fabricate efficient phosphorescent dye doped polymer light emitting devices. © *2003 American Institute of Physics.* [DOI: 10.1063/1.1535211]

I. INTRODUCTION

Operation of polymer light emitting diodes (LEDs) brings electrons and holes from opposite electrodes and generates singlet and triplet excitons. Until recently, polymer LEDs have utilized fluorescence from singlet excitons only. Triplet excitons are wasted because a radiative decay from triplets is spin-forbidden and often very inefficient. Spin statistics predicts that singlet-to-triplet ratio is 1:3 in organic semiconductors and it is experimentally verified recently.[1,2] The ratio in π-conjugated polymers has been investigated during the last couple of years and recent studies revealed that singlet formation rate can be as high as 50% or even higher.[2–5] The high ratio was attributed to the larger formation cross section of singlet than triplet exciton due to delocalization nature of charged particles in π-conjugated polymers. Even though the singlet ratio in π-conjugated polymers might be higher than the prediction by spin statistics, utilization of triplet excitons will increase the light emission efficiency significantly in polymer LEDs.

One way to harvest light from triplet excitons is to use phosphorescent dyes.[2,6–23] These materials incorporate a heavy metal atom to mix singlet and triplet states by the strong spin–orbit coupling. As a result, a spin forbidden transition may occur allowing an enhanced triplet emission. Lanthanide and transition metal complexes have been used as phosphorescent dyes and they are incorporated in an organic molecule or in a polymer as a dopant. Among them, transition metal complexes such as 2,3,7,8,12,13,17,18-octaethyl-21H,23H-porphyrin platinum(II) (PtOEP) and *fac* tris(2-phenylpyridine) iridium [$Ir(ppy)_3$] have attracted attention because of the short triplet lifetime to minimize the triplet–triplet annihilation.[6,7] High quantum efficiencies were obtained by doping $Ir(ppy)_3$ or PtOEP in organic molecules[14–16] and in polymers.[17–23]

Even though high emission efficiencies and many phosphorescent dyes have been reported during the last couple of years, less attention has been paid on the energy transfers, especially, in polymer LEDs. Baldo *et al.* investigated triplet–triplet energy transfer in phosphorescent organic LEDs by comparing transient electroluminescence with and without reverse bias after a short electrical excitation pulse and found the evidences of triplet–triplet energy transfer for

a)Electronic mail: jjk@kjist.ac.kr

 © 2003 American Institute of Physics

Downloaded 24 Mar 2008 to 68.181.190.164. Redistribution subject to AIP license or copyright; see http://jcp.aip.org/jcp/copyright.jsp

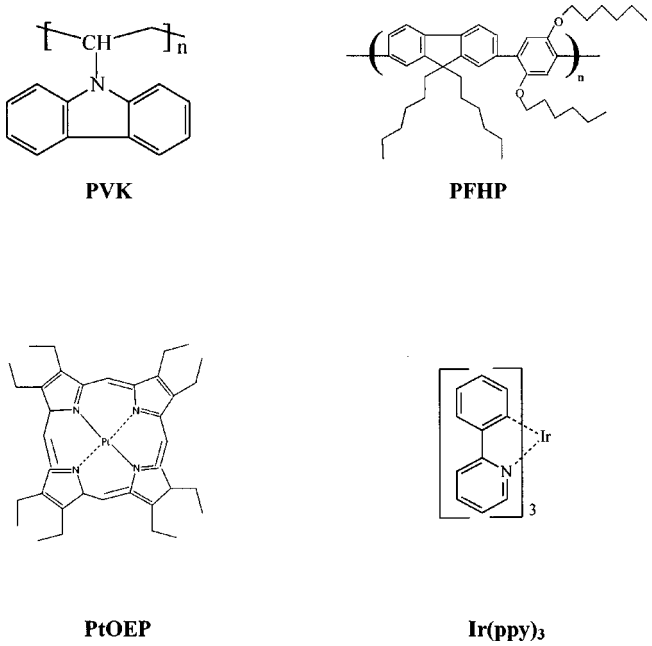

FIG. 1. Chemical structures of host polymers and phosphorescent dyes used in this work.

some combination of guests and hosts.[24] Cleave *et al.* observed the existence of triplet–triplet energy transfer from poly[4-(*N*-4-vinylbenzyloxyetyl, *N*-methylamino)-*N*-(2,5-di-*tert*-butyl phenylnaphthalimide)] (PNP) to PtOEP by a time-resolved electroluminescence (EL) experiment.[17] On the other hand, Lane *et al.* could not observe the triplet-triplet energy transfer from poly (9,9-dioctylfluorene) (PFO) to PtOEP by investigating modulation frequency dependence of photoinduced absorption (PA) signal.[20]

An efficient polymer based LED necessitates the development of suitable polymeric materials that can achieve an effective energy transfer via Förster or Dexter mechanism between the polymer host and the phosphorescent guest. The hole and electron trapping by the dopant and the subsequent dopant/matrix carrier recombination is also a significant contributor to the overall EL emission from polymer based LEDs.[17,20] The above examples indicate that the singlet and triplet energy transfer are not automatically guaranteed even though the conventional requirements for the energy transfers are satisfied in phosphorescent dye doped polymer systems from a certain host polymer to a phosphorescent dyes.

In this paper, we elucidate the triplet–triplet and singlet–singlet energy transfer between polymer hosts and phosphorescent dyes by investigating the triplet exciton dynamics for different host–guest luminescence systems. We selected poly(*N*-vinylcarbazol) (PVK) and poly[9.9′-di-*n*-hexyl-2,7-fluorene-alt-1,4-(2,5-di-*n*-hexyloxy)phenylene] (PFHP) as donor polymers and two phosphorescent dyes, $Ir(ppy)_3$ and PtOEP, as acceptor molecules. Figure 1 shows the molecular structure of polymers and phosphorescent dyes used in this study. PVK is a polymer with luminescent side chain chromophore and PFHP is a π-conjugated polymer, respectively. The polymers were selected as the host materials because emission spectra of both polymers have the good spectral overlap with the metal-ligand-charge-transfer (MLCT) absorption spectrum of $Ir(ppy)_3$ and *Q* and *B* absorption bands of PtOEP so that efficient Förster energy transfers are expected. If T_1 of the polymers has the similar separation from S_1 as estimated by the reported results in π-conjugated polymers,[25]

$$T_1 = (1.13S_1 - 1.43) \pm 0.25 \text{ eV}, \tag{1}$$

we can expect good spectral overlaps between the triplet emission spectrum of the hosts and the singlet ground state to first triplet excited state absorption of the guest, $Ir(ppy)_3$. Therefore, efficient Dexter transfer is expected from the polymers to the guest.

We employed two methods to investigate the triplet energy transfer: (1) comparing the dynamics of the lowest excited triplet state of the host polymer between the doped and undoped films,[20] and (2) comparing the transient electroluminescence response between the doped and undoped polymer LEDs.[17,24] The first method is valuable to directly probe the triplet energy transfer for the system in which T_1 of a host material has much longer lifetime than that of a guest. This is the case for our system. The lifetime of the triplet state of the guest is shorter than 100 μs for PtOEP and 1 μs for $Ir(ppy)_3$, whereas triplet lifetimes of π-conjugated polymers are generally in the range of 100 μs to a few milliseconds.[20,25,26] If triplet energy transfer takes place from the host to the guest in the system, the triplet lifetime of the host will be shortened by doping because of the opening of the fast decay channel.[20] For the purpose, the T_1 level of the host polymers was determined first, and then the decay dynamics of the phosphorescence of the host polymers was compared between the neat and phosphorescent dye doped polymers. The second method was employed to probe the triplet energy transfer in LEDs as a complementary method. The method is well described in literatures.[17,24]

The description of our investigations includes the experimental methods in Sec. II, the identification the phosphorescence from the delayed fluorescence of the hosts in Sec. III, and the triplet–triplet and singlet energy transfer in the phosphorescent dye doped polymer LEDs in Secs. IV and V, respectively. The reason for the different behavior of the energy transfer in different host polymers will be discussed based on the morphological investigation of the dye doped polymer systems in Sec. VI. The effect of different polymer systems on devices performance is finally described in Sec. VII followed by a summary in Sec. VIII.

II. EXPERIMENTAL METHODS

$Ir(ppy)_3$ was synthesized according to the literature[27] and PFHP was synthesized by Suzuki coupling process in KIST (Korean Institute of Science and Technology). Other chemicals were purchased from Kanto (PVK), Porphyrin Products Inc. (PtOEP), Bayer [PEDOT (poly(3,4-ethylene dioxythiophene))], and Syntec (TAZ and Alq_3). The films for room and low temperature photoluminescence (PL) experiments were formed on pre-cleaned quartz plate (Hellma) at air atmosphere. PVK and PFHP were dissolved in 1.2-dichloroethane and *p*-xylene, respectively, at a concentration of 10 mg/1 g. Room temperature photoluminescence spectra were detected by an ACTON spectrometer (SpectraPro-300i)

Downloaded 24 Mar 2008 to 68.181.190.164. Redistribution subject to AIP license or copyright; see http://jcp.aip.org/jcp/copyright.jsp

connected with a photomultiplier tube (Acton Research, PD-438). A xenon lamp was used as the excitation source connected with other monochrometer (SpectraPro-150i). Absorption spectra were recorded on a Hewlett-Packard HP8452A UV-visible diode array spectrophotometer.

Low temperature PL spectra were obtained by the fourth harmonic of a Q-switched Nd-YAG laser using the upper excite state energy transfer[28] with a pulse duration of 6 ns and a repetition rate of 10 Hz. The laser beam had a diameter of 5 mm and an optical power of ~50 mJ. The emission from the film in a cryostat flowing condensed helium gas was recorded by a gated intensified diode array detector through a monochromator. The system allows for an integration time (gate width) of detection from 100 ns to 10 ms and a variable delay after excitation.

The LEDs have the structure of ITO/ PEDOT (40 nm)/ Host-Ir$(ppy)_3$ (30 nm)/TAZ (30 nm)/Alq_3 (20 nm)/LiF (0.5 nm)/Al (200 nm). Current–voltage–luminescence characteristics of the devices were obtained using a Keithley 237 Source Measurement Unit and a calibrated silicon photodiode connected with an optical power meter (Newport 1835-C). For the time resolved EL measurements, a current pulse from a function generator (HP 8116A) triggered with a storage-sampling oscilloscope (Tektronics TDS520B) was applied to the LEDs. The pulses had the width of 100–200 ns and the repetition rate of 100 Hz. The decay signals were monitored by the two-channel oscilloscope and averaged more than 1000 times to reduce the noise. The emitted light from the EL device was collected by a fast response photomultiplier tube (2 ns). The RC time constant of the device was about 45 ns, which is a sufficiently small value not to distort the transient measurements.[24,29,30]

Microstructures of dye doped polymer films were investigated using a transmission electron microscope (TEM, Carl-Zeiss LEO EM-912 equipped with an Omega-type energy filter at an accelerating voltage of 120 kV), an atomic force microscope (AFM, NanoScope III, Digital Instrument, Inc.), and a fluorescence microscope (FM, Olympus BX-51 with a 100 W mercury lamp). Specimens for TEM observation were prepared as follows: The polymer solutions doped with Ir$(ppy)_3$ were cast on an air-cleaved potassium chloride (KCl) surface and then reinforced by the plasma-polymerized osmium tetraoxide. The thin film on KCl was then stripped from the substrate and then transferred to a copper mesh.

AFM measurements were performed in air at room temperature. A Si_3N_4 cantilever with a spring constant of 0.12 N/m was used at a scanning rate of 2–3 Hz. The applied force was minimized during the AFM imaging by adjusting the ''set-point voltage'' to the lower limit.

III. DELAYED FLUORESCENCE AND PHOSPHORESCENCE

Low temperature, time resolved spectroscopy technique was employed to determine the triplet energy levels and thereby to investigate the dynamics of the triplet excitons of host polymers. Figure 2(a) shows the delayed luminescence spectra of PFHP at 5.5 K recorded with delay times of 5, 20, and 40 μs, respectively. The spectra consist of three contributions. The high-energy portion (I) appears in the same wavelength region as the prompt fluorescence [inset of Fig. 2(a)] with a maximum near 430 nm. It is therefore ascribed to delayed fluorescence (DF). The second contribution (II) centered at 508 nm appears also in the same wavelength range of the excimerlike band in the prompt fluorescence. The third contribution (III) centered at 540 nm is resolved only in the delayed luminescence at low temperature and at the integration times larger than 20 μs. It overlaps with the relatively strong excimerlike band (II) and is masked by the band at short delay time of 5 μs. The emission peak of 540 nm (2.3 eV) agrees with a value obtained using a pulsed radiolysis method for the triplet energy of polyfluorene.[25] Therefore we assign the emission centered at 540 nm to be the phosphorescence (Ph) from the spin forbidden $S_0 \leftarrow T_1$.

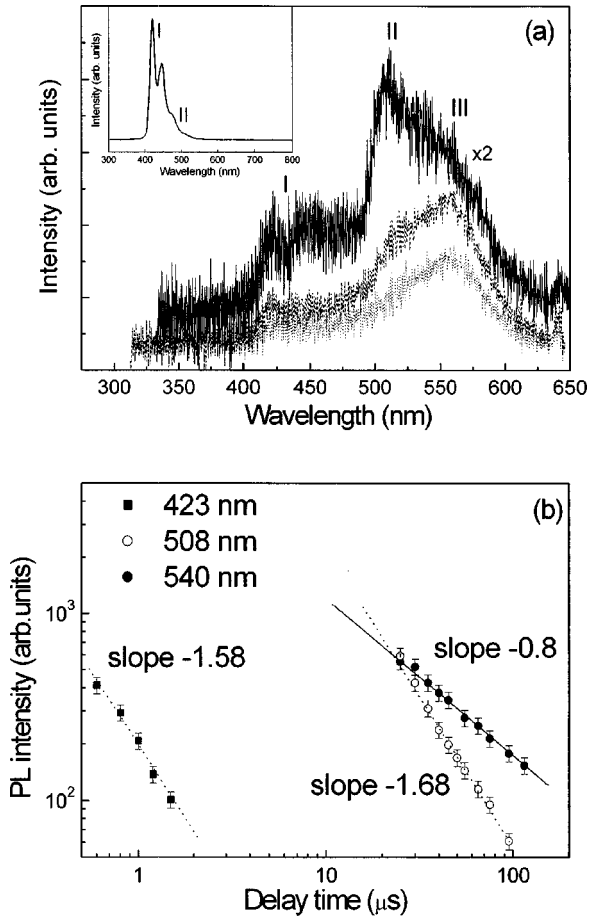

FIG. 2. (a) The photoluminescence spectra of PFHP with different gate width (1, 50, and 50 μs from top to bottom) and delay time (5, 20, and 40 μs from top to bottom) at low temperature (5.5 K). Inset: the prompt photoluminescence spectra of PFHP. (b) Decay curves of delayed fluorescence at 423 nm (filled squares, integration time=100 ns), 508 nm (opened circles, integration time=10 ms) and phosphorescence at 540 nm (filled circles, integration time=10 ms) of PFHP on the double logarithmic scale.

Decay kinetics of the DF, excimer emission (EE), and phosphorescence (Ph) has been investigated. For this purpose, we separately integrated the spectral contributions after recoding the luminescence at various delay times and gate widths. The results are shown in Fig. 2(b) on a double logarithmic scale. All the emissions decay in power law fashions

Downloaded 24 Mar 2008 to 68.181.190.164. Redistribution subject to AIP license or copyright; see http://jcp.aip.org/jcp/copyright.jsp

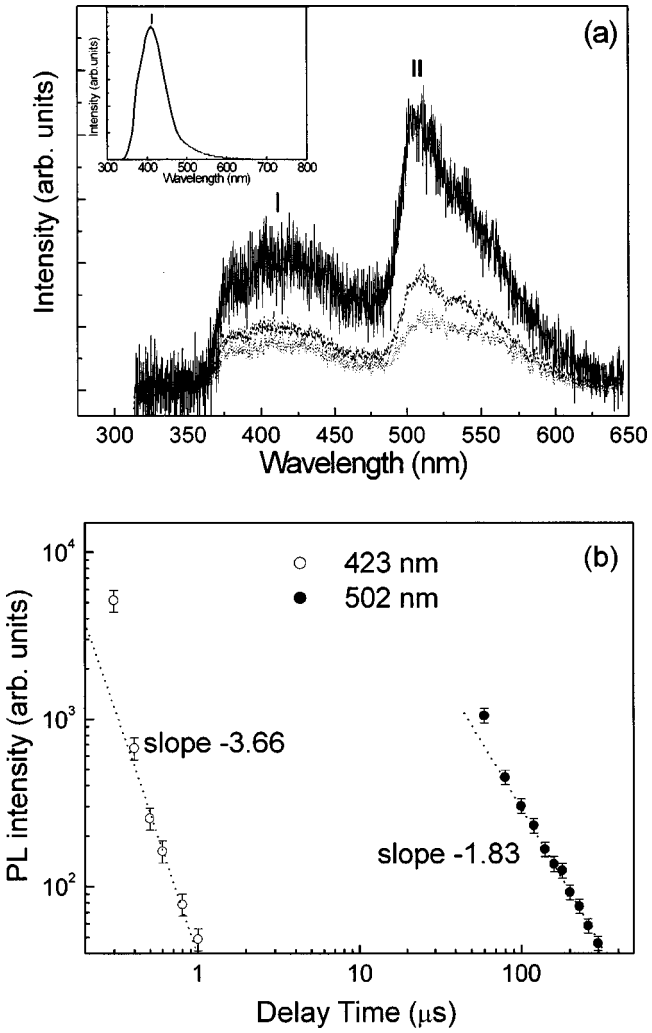

FIG. 3. (a) The photoluminescence spectra of PVK with different gate width (1, 50, and 50 μs from top to bottom) and delay time (5, 20, and 40 μs from top to bottom) at low temperature (5.5 K). Inset: the prompt photoluminescence spectra of PVK. (b) Decay curves of delayed fluorescence at 423 nm (opened circles, integration time=100 ns), and phosphorescence at 502 nm (filled circles, integration time=10 ms) of PVK on the double logarithmic scale.

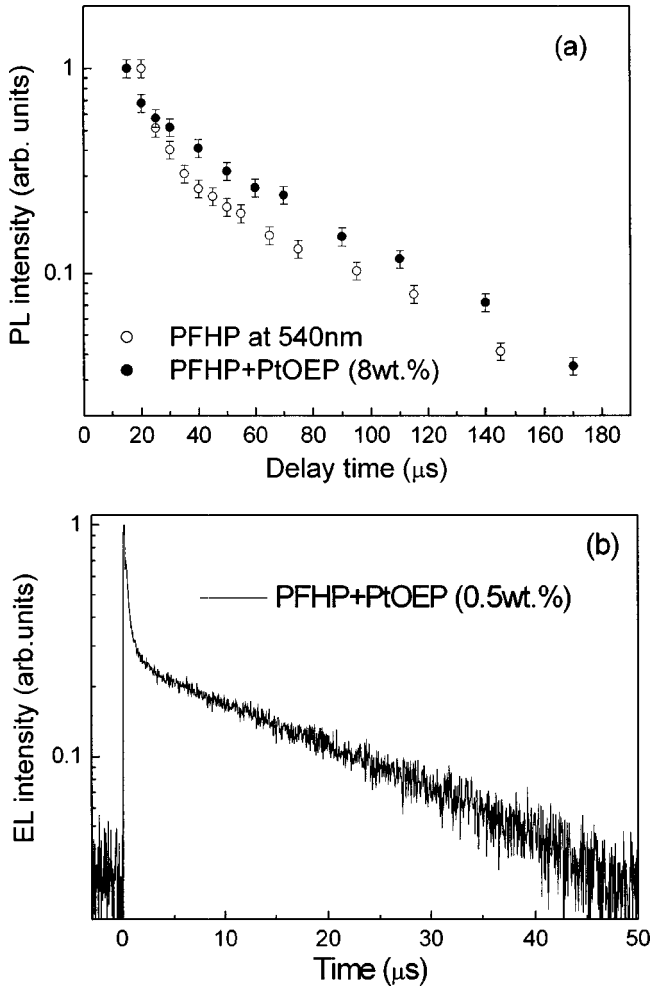

FIG. 4. (a) Decay profiles of the T_1 state of PFHP (opened circles) and PtOEP doped PFHP (filled circles) films at 540 nm measured at 5.5 K. (b) EL response of PtOEP doped PFHP device after a short rectangular pulse (15 V, 200 ns) followed by a reverse bias (-15 V).

with slopes of -1.6, -1.7, and -0.8 for DF, EE, and Ph, respectively. It is important to note that decays of EE and Ph are the integrated kinetics as we used the integration time of 10 ms. In this case the true kinetics is a derivative of the integrated kinetics and obeys power laws with the $\sim t^{-2.7}$ decay for the EE and $\sim t^{-1.8}$ for the Ph, respectively. In contrast, the decay for DF is the real kinetics with $\sim t^{-1.6}$ because the integration time was 100 ns that is much shorter than delay times.

Origin of the power law dependence of the DF and Ph decay in PFHP is not clearly understood yet. However, the power law dependence of DF and Ph decay seems to be general in conducting polymers. A few groups recently reported the same behavior for DF and Ph in different conducting polymers of MeLPPP, PMOT, and Ph2/6.[26,31,32] They suggested that the origin of the DF is delayed germinate pair recombination rather than triplet–triplet annihilation. If the latter mechanism described the reality then linear and quadratic slopes in a semilogarithmic plot are expected for Ph and DF, respectively, since the annihilation of two triplets generates only one singlet exciton. The origin of the power law dependence of DF, EE, and Ph in PFHP is under study now.

Similar experiments were performed for PVK. Figure 3(a) shows the delayed luminescence spectra of PVK recorded with various integration times and delay times at 5.5 K. The spectra consist of two contributions. The high-energy portion (I) appears in the same wavelength range as the prompt fluorescence [inset of Fig. 3(a)] so that we ascribe it to the delayed fluorescence. The second spectral contribution (II) peaked at 502 nm (2.46 eV) is only observed in delayed luminescence and has a similar shape to the fluorescence, but is offset from the latter by about 90 nm. Therefore we assign the contribution to phosphorescence. DF and Ph of PVK decay in power law fashions as shown in Fig. 3(b). Again the measured decay of Ph corresponds to the integration kinetics. The real decay kinetics obeys power law of $\sim t^{-2.8}$ for Ph and $\sim t^{-3.7}$ for DF, respectively.

The location of triplet state of PFHP (2.3 eV) and PVK (2.46 eV) are relatively well matched with T_1 calculated by Eq. (1) and both decay profiles of T_1 show much longer

Downloaded 24 Mar 2008 to 68.181.190.164. Redistribution subject to AIP license or copyright; see http://jcp.aip.org/jcp/copyright.jsp

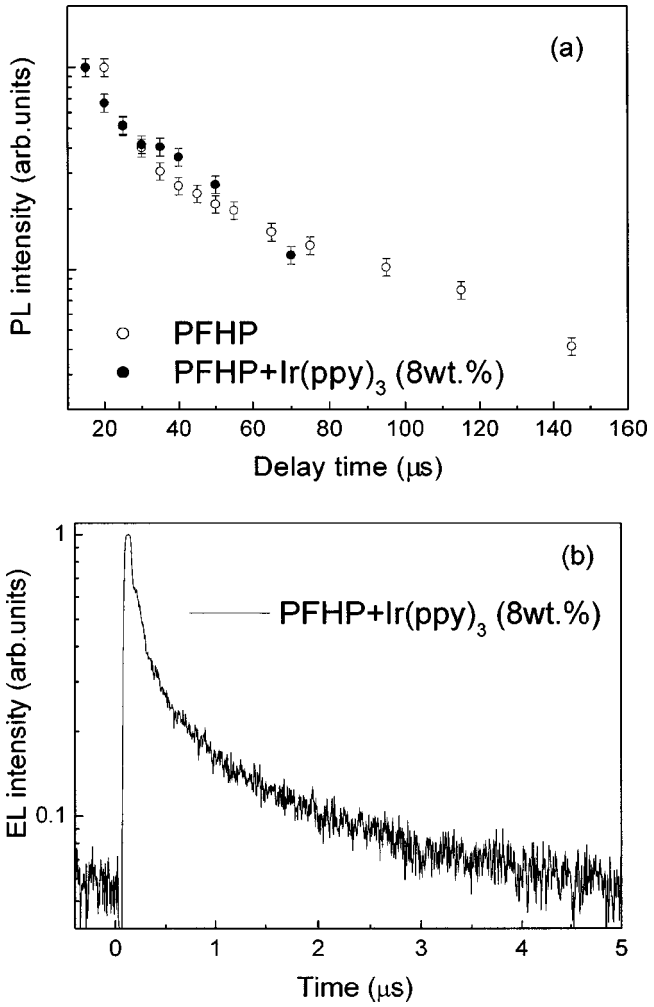

FIG. 5. (a) Decay profiles of the T_1 state of PFHP (opened circles) and $Ir(ppy)_3$ doped PFHP (filled circles) films at 540 nm measured at 5.5 K. (b) EL response of $Ir(ppy)_3$ doped PFHP device after a short rectangular pulse (13 V, 200 ns) following by a reverse bias (-13 V).

lifetime than 100 μs. This result indicates that a polymer with emissive side chain chromophore such as PVK shows the large splitting between S_1 and T_1 similar to π-conjugated polymers. It is not conclusive yet whether the large difference is a general character of the side chain polymers. However, we can conjecture at least, that the electron–electron interaction can be large because of the localized excited states in the polymer that leads to a large gap between S_1 and T_1 of PVK.[25,26]

IV. TRIPLET–TRIPLET ENERGY TRANSFER

Figure 4(a) shows the decay profiles of the phosphorescence peaks from the films of neat PFHP and PFHP doped with PtOEP (8 wt. % of PFHP). Each point was detected with the same gate width (integration time) to avoid a deformation of decay pattern by the change of experimental condition. As shown in Fig. 4(a), two films show almost the same decay rate except the initial fast decreasing band, which is due to the fast quenching through triplet–triplet annihilation.[26] Thus, we found that the doping of PtOEP had little influence on the lifetime of T_1 of PFHP and it indicates that the

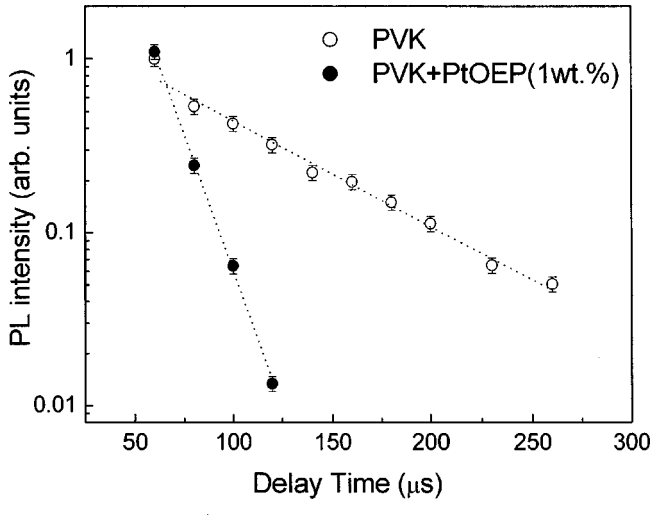

FIG. 6. Decay profiles of the T_1 state of PVK (opened circles) and PtOEP doped PVK (filled circles) films at 502 nm measured at 5.5 K. The triplet lifetime of PVK at 502 nm was shortened by doping of PtOEP.

triplet–triplet energy transfer does not occur from T_1 of PFHP to T_1 of PtOEP even at the high doping concentration. This consequence is consistent with the result of transient EL response of the LED having the PtOEP doped PFHP as the emitting layer. In the experiments, we applied the reverse bias of -15 V as soon as the voltage pulse is off in order to remove residual charge carriers injected by the electrical pulse, thereby to prevent a recombination directly on the dopant.[17,24] Figure 4(b) shows the time resolved EL response of PtOEP doped PFHP at the concentration of 0.5 wt. %. At this concentration, both blue emission from PFHP and red emission from PtOEP are observed at the same time. The fast initial peak in Fig. 4(b) is induced by blue emission from PFHP, which has the lifetime of several hundred picoseconds. However, the delayed phosphorescence, an evidence of Dexter energy from triplet of PFHP to PtOEP, was not observed. Therefore, we conclude that the triplet energy transfer is absent in PtOEP:PFHP system even though the T_1 state of PFHP is located higher than that of PtOEP.

Figure 5(a) compares the decay profiles of the phosphorescence peak from neat PFHP and $Ir(ppy)_3$ doped PFHP films. The features of two decays rarely show any difference. Moreover, as shown in Fig. 5(b), the transient EL response did not show the delayed phosphorescence similar to the device of PtOEP doped PFHP. In case of the film of $Ir(ppy)_3$ doped PFHP, the π-conjugated polymer has lower T_1 energy level (2.3 eV) than that of $Ir(ppy)_3$ (2.4 eV). This condition is a little unfavorable for triplet energy transfer. However, Dexter energy transfer can still be possible in the system ($\Delta G \sim +0.1$ eV). Adachi *et al.* reported efficient triplet–triplet energy transfer in the system ($\Delta G \sim +0.06$ eV), where host CBP has a lower T_1 state than guest Iridium(III)bis[4,6-di-fluorophenyl-pyridinato-N,$C^{2'}$] Picolinate (Flrpic) via an endothermic energy transfer.[13]

The same measurements were conducted for PVK as host and $Ir(ppy)_3$ and PtOEP as guests. Figure 6 shows the decay profiles of the phosphorescence spectrum (502 nm) of the neat PVK film and a PtOEP:PVK system. The decay of

Downloaded 24 Mar 2008 to 68.181.190.164. Redistribution subject to AIP license or copyright; see http://jcp.aip.org/jcp/copyright.jsp

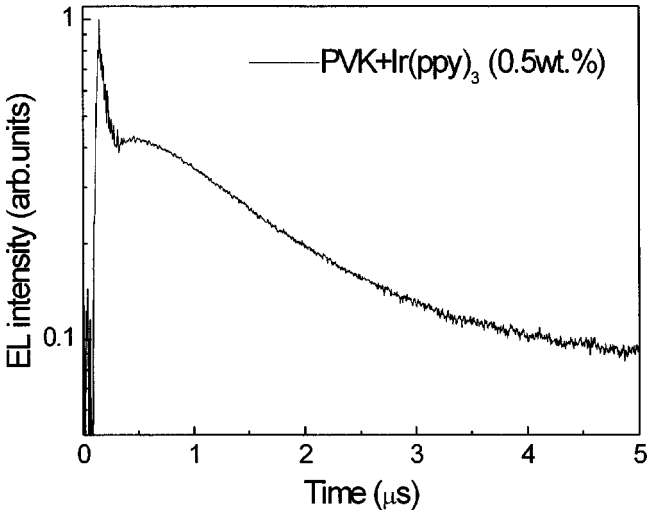

FIG. 7. EL response of $Ir(ppy)_3$ doped PVK device after a rectangular pulse (16 V, 200 ns) followed by a reverse bias (-16 V). The operation of Dexter energy transfer was confirmed by the initial rise.

phosphorescence intensity of PVK becomes much faster by doping PtOEP in the film. The shortening of the T_1 lifetime of the host by doping PtOEP suggests the opening of a new fast decay channel of the T_1 state of PVK. It is a clear evidence on the existence of the triplet–triplet energy transfer from PVK to PtOEP. In the $Ir(ppy)_3$:PVK system, however, we could not separate the phosphorescence spectrum of PVK from the phosphorescence emission of $Ir(ppy)_3$ because of their spectral overlap. So, we could only examine the triplet energy transfer by the transient EL measurement with reverse bias. Figure 7 shows the EL decay pattern after the short electrical pulse (200 ns) followed by a reverse bias. It clearly shows the intensity increment after the fast decay within a few hundred nanoseconds. The increment of EL intensity should be originated from the excitation transferred by both Förster and Dexter mechanism. The possibility of charge trapping of remaining charge carriers on dopant site is discarded since the reverse bias of -16 V was applied quickly after the 16 V forward bias pulse to remove the remaining charge carriers.[17] This result supports the efficient triplet–triplet energy transfer from T_1 of PVK to T_1 of $Ir(ppy)_3$. Thus the study of triplet exciton dynamics provides experimental evidences of the efficient triplet energy transfer in PtOEP:PVK and $Ir(ppy)_3$:PVK systems in contrast to PFHP systems.

V. SINGLET ENERGY TRANSFER

Figure 8(a) shows the absorption spectrum of a film of $Ir(ppy)_3$ (solid line), and emission spectra of PVK (dashed line), and PFHP (dotted line). Both PFHP and PVK showed the large spectral overlap with the absorption of ^{1}MLCT of $Ir(ppy)_3$. We calculated the Förster transfer radius from Fig. 8(a).[33,34] It is defined as the characteristic distance between a host and a guest at which the efficiency of energy transfer is 50%. The Förster radii were 31.7 and 30.7 Å for $Ir(ppy)_3$:PVK and $Ir(ppy)_3$:PFHP systems, respectively. Thus, efficient singlet energy transfers are expected for both the systems. Figure 8(b) shows normalized PL spectra of films made of 8 wt. % of $Ir(ppy)_3$ in PVK (solid line) and in PFHP (dashed line). The excitation wavelength for the PL measurements was 318 nm, where the absorption by $Ir(ppy)_3$ is minimal so that most of the excitation light is absorbed by the hosts. The luminescence spectrum from $Ir(ppy)_3$:PVK system is the same as that of $Ir(ppy)_3$, indicating an efficient singlet energy transfer in the system. In contrast, most of the emission comes from the host (PFHP) in $Ir(ppy)_3$:PFHP system, implying that the singlet energy transfer does not take place from PFHP to $Ir(ppy)_3$ even though the Förster radius is almost the same as the $Ir(ppy)_3$:PVK system. Figure 8(c) shows the absorption spectrum of PtOEP and emission spectra of PVK and PFHP and Fig. 8(d) shows the emission spectra of the PtOEP (8 wt. %): PVK and PtOEP (8 wt. %): PFHP systems, respectively. Excitation wavelength of 350 nm was used for the systems. Similar to the $Ir(ppy)_3$ doped systems, singlet energy transfer is efficient, if PtOEP is doped in PVK. However, it is inefficient in PFHP. We conclude from the results that Förster and Dexter energy transfer take place efficiently in $Ir(ppy)_3$:PVK and PtOEP:PVK systems, but $Ir(ppy)_3$:PFHP and PtOEP:PFHP systems show very weak energy transfers.[35] This is a rather surprising result because PVK and PFHP have almost the same emission spectrum and both of them have large Förster radius with $Ir(ppy)_3$.

Polyfluorene and its derivatives are known as materials forming aggregates which prohibit a sufficient close contact for exciton transfers between the host and guest molecules.[36,37] In an analogous way, if the aggregation in PFHP is the reason of preventing the energy transfer(s) due to the chain-packing effect, the energy transfer(s) should be observed in the nonaggregated form of the host. We employed two methods to untangle the aggregation of PFHP: (1) blending of PFHP with an inert polymer PMMA (polymethyl methacrylate) and (2) preparing solution with good solvent such as *p*-xylene. The lifetime of the film of PFHP was found to increase when PFHP was blended with PMMA. Thus it is pertinent that an aggregation is minimized when the doped system is blended with PMMA. Figure 9(a) shows normalized PL spectra of films made of PMMA: PFHP: $Ir(ppy)_3$ with different PMMA to PFHP ratios. $Ir(ppy)_3$ to PFHP ratio was maintained at 6 wt. % for all the films. The green emission from $Ir(ppy)_3$ was observed from the blended films. The green emission must be induced by the energy transfer probably as a consequence of the reduction of aggregation of PFHP. It is not induced by the self-excitation of $Ir(ppy)_3$ because its concentration in the blended films is lower than the unblended films. Figure 9(b) shows that the PL spectra of the solution PFHP and $Ir(ppy)_3$ (8 wt. % of the host) dissolved in *p*-xylene (10.8 mg of /1 g of solvent). The green emission from $Ir(ppy)_3$ again substantiates the fact that energy can be transferred from a much less aggregated PFHP in solution to the phosphor. Since the blending and the solution untangle the aggregation of the host, the apparent absence of energy transfer in PFHP is likely to be related to the aggregation of PFHP in question.

Downloaded 24 Mar 2008 to 68.181.190.164. Redistribution subject to AIP license or copyright; see http://jcp.aip.org/jcp/copyright.jsp

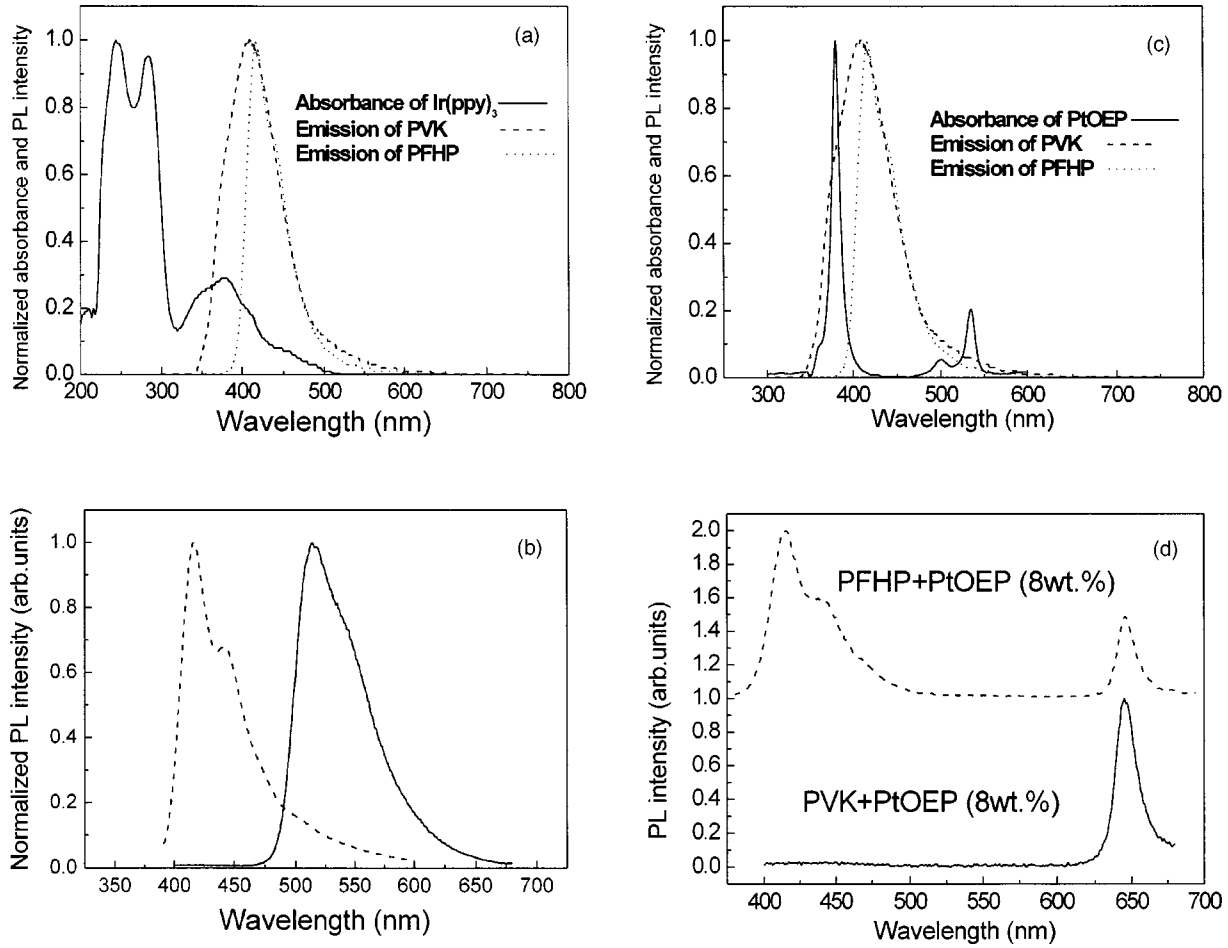

FIG. 8. (a) Absorption spectrum of the film of $Ir(ppy)_3$ (solid line) and emission spectra of PVK (dashed line, $\lambda_{exc}=350$ nm) and PFHP (dotted line, $\lambda_{exc}=380$ nm) films. (b) Normalized PL spectra from 8 wt. % $Ir(ppy)_3$ doped PVK (solid line) and PFHP (dashed line) films, respectively. The films were excited with 318 nm light where the absorbance of $Ir(ppy)_3$ is minimum. (c) Absorption spectrum of PtOEPfilm (solid line) and emission spectra of PVK (dashed line, $\lambda_{exc}=350$ nm) and PFHP films (dotted line, $\lambda_{exc}=380$ nm), respectively. (d) PL spectra from PtOEP doped (8 wt. %) PVK (solid line) and PFHP (dashed line) films, respectively. The films were excited with 350 nm light so that most of the excitation light is absorbed by the hosts.

VI. MICROSTRUCTURE OF $Ir(ppy)_3$ DOPED POLYMER FILMS

More direct evidences of aggregate formation in $Ir(ppy)_3$ doped PFHP films were obtained from TEM, AFM, and fluorescence microscope (FM) images. Figures 10(a) and 10(b) show TEM images of freestanding films (thickness $\sim$20 nm) of PFHP and PVK doped with $Ir(ppy)_3$ (8 wt. % of the hosts), respectively. The PFHP:$Ir(ppy)_3$ film shows the aggregate domains on length scales of 50–200 nm [Fig. 10(a)]. Since the iridium atom has a larger electron scattering cross section than the carbon atom, the dark spots are likely to be $Ir(ppy)_3$ aggregates, even though the chemical composition of the aggregated domains has not yet been clarified. On the other hand, the PVK:$Ir(ppy)_3$ film shows a featureless image [Fig. 10(b)], suggesting that the film is homogeneous with no phase separation or aggregates.

The surface topographies of the films were investigated by AFM and are displayed in Fig. 11. The PFHP:$Ir(ppy)_3$ film shows an aggregated domain with a horizontal size of $\sim$250 nm and a vertical roughness in the range of $\pm$25 nm as shown in Fig. 11(a). In contrast, the PVK:$Ir(ppy)_3$ film is smooth with the height variation in the range of less than $\pm$1 nm as shown in Fig. 11(b), suggesting that the film is homogeneous with no phase separation or aggregates.

Large scale images of $Ir(ppy)_3$ doped polymer films were obtained using a fluorescence microscope (FM). In order to observe images by the FM, doping concentration of $Ir(ppy)_3$ in PVK and PFHP films was increased to 15 wt. % to enlarge the aggregates it there are. Figures 12(a) and 12(b) display the images of $Ir(ppy)_3$:PFHP, and Figs. 12(c) and 12(d) the image of $Ir(ppy)_3$:PVK, respectively. Figures 12(a) and 12(c) were obtained under the excitation light of the spectral range of 330–385 nm with 420 nm barrier filter to avoid direct detection of the excitation light and Figs. 12(b) and 12(d) and under the excitation of spectral range of 460–490 nm with 520 nm barrier filter for the same purpose, respectively. Both $Ir(ppy)_3$ and the hosts PVK and PFHP will be excited by the light of 330–385 nm because they have strong absorption in the range. In contrast, only $Ir(ppy)_3$ will absorb light in the range of 460–490 nm because there is no absorption by the hosts in the range.

Figure 12(a) shows green emissive needlelike images in blue background. The blue background corresponds to the

Downloaded 24 Mar 2008 to 68.181.190.164. Redistribution subject to AIP license or copyright; see http://jcp.aip.org/jcp/copyright.jsp

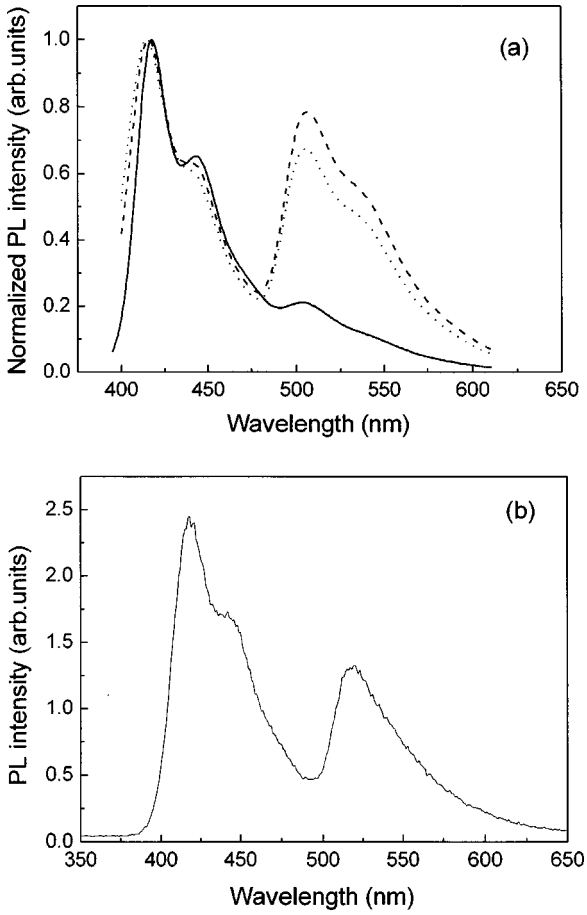

FIG. 9. (a) Normalized photoluminescence spectra of films made of PMMA (1): PFHP: (1): $Ir(ppy)_3$ (0.06) (solid line), PMMA (1): PFHP (0.5): $Ir(ppy)_3$ (0.03) (dashed line) and PMMA (1): PFHP (0.025): $Ir(ppy)_3$ (0.015) (dotted line). All films were excited with light at 318 nm where the absorbance of $Ir(ppy)_3$ is minimum.(b) Photoluminescence spectrum of PFHP and $Ir(ppy)_3$ (8 wt. % of host) solution dissolved in *p*-xylene [10.8 mg of PFHP and $Ir(ppy)_3$/1 g of solvent].

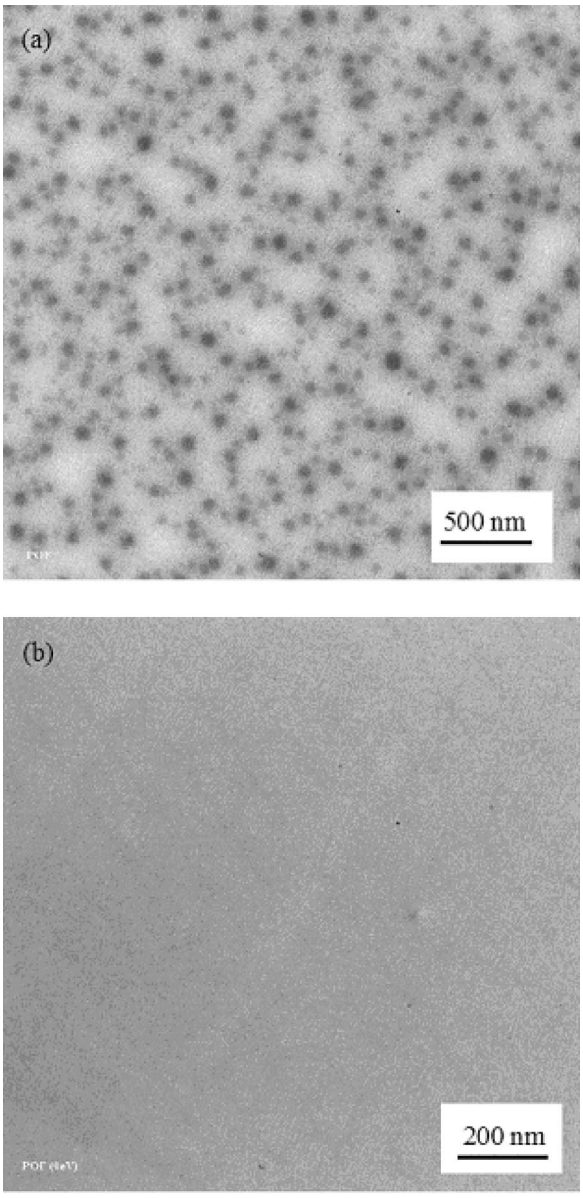

FIG. 10. TEM image of films of (a) $Ir(ppy)_3$ (8 wt. %) doped in PFHP shows aggregates unlike the (b) $Ir(ppy)_3$ film (8 wt. %) doped in PVK.

fluorescence from PFHP. When the film is excited with the light of 460–490 nm, the needle shapes emit bright green in dark background which indicates that the needle shapes are composed of $Ir(ppy)_3$ and the background contains a little amount of $Ir(ppy)_3$. Figures 12(a) and 12(b) clearly demonstrate that $Ir(ppy)_3$ forms aggregates in PFHP. It is quite common that morphology of aggregates changes with doping concentration. Generally, the aggregates have spherical shape at low doping concentration. As the doping concentration increases, the aggregates coalesce to grow into various forms like dendrite or needle shapes. Therefore, it is not surprising to observe that the aggregates have spherical shape at the low concentration of 8 wt. % (TEM images) and needle shape at high concentration of 15 wt. %.

In contrast, $Ir(ppy)_3$:PVK films exhibit homogeneous, featureless green images independent of excitation wavelength [Fig. 12(c)]. The green emission without blue emission from the film when excited with the light of 330–385 nm results from the energy transfer from PVK to $Ir(ppy)_3$. The images of Figs. 12(c) and 12(d) demonstrate homogeneous dispersion of $Ir(ppy)_3$ in PFHP within the resolution of the FM and efficient energy transfer from PVK to $Ir(ppy)_3$. In summary, all the TEM, AFM and FM images clearly show that $Ir(ppy)_3$ is homogeneously dispersed in PVK, but it forms aggregates in PFHP.

VII. DEVICE PERFORMANCE

EL spectra of PFHP:$Ir(ppy)_3$ are compared with PL spectra for different doping concentrations in Fig. 13. PL spectra of PFHP:$Ir(ppy)_3$ films show only a blue emission from PFHP even at high doping concentrations as shown in Fig. 13(a) since singlet energy transfer does not take place from PFHP to $Ir(ppy)_3$. The EL spectrum changes with doping concentration as shown in Fig. 13(b) and the applied voltage at the same doping concentration (not shown). Most of the light was emitted from PFHP in the EL devices when the doping concentration was lower than 2%. In contrast, light was mostly emitted from $Ir(ppy)_3$ if the doping is higher than 8%. This fact indicates that the light was emitted

Downloaded 24 Mar 2008 to 68.181.190.164. Redistribution subject to AIP license or copyright; see http://jcp.aip.org/jcp/copyright.jsp

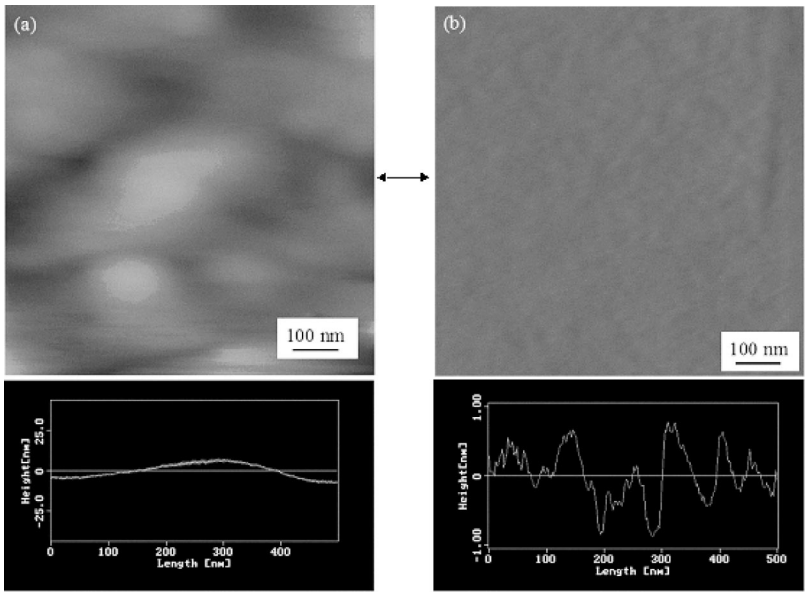

FIG. 11. AFM images of the surfaces of (a) PFHP:Ir(ppy)$_3$ (8 wt. %), (b) PVK:Ir(ppy)$_3$ (8 wt. %). The corresponding cross sections of the surface heights of the thin films were taken horizontally from the point indicated by an arrow.

by direct charge trapping and recombination on the dye molecules at the high doping concentrations since the singlet and triplet energy transfer did not take place in the PFHP:Ir(ppy)$_3$ film. HOMO (highest occupied molecular orbital) and LUMO (lowest unoccupied molecular orbital) levels of the PFHP and Ir(ppy)$_3$ are aligned favorably for the charge confinement. The HOMO levels of PFHP and Ir(ppy)$_3$ are 5.7 and 5.5 eV and LUMO levels are 2.7 and 3.0

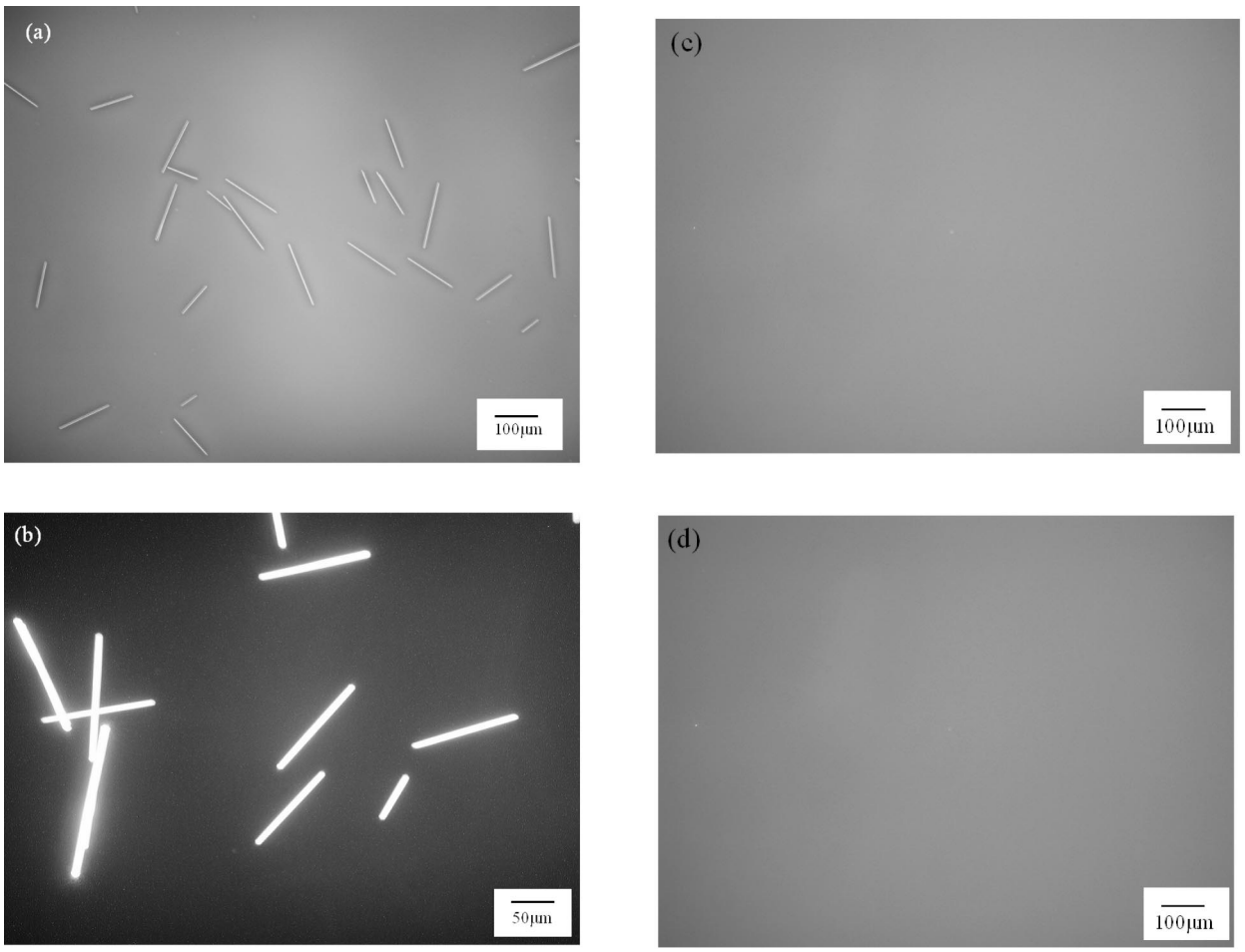

FIG. 12. Fluorescence micrographs of PFHP:Ir(ppy)$_3$ [(a), (b)] and PVK:Ir(ppy)$_3$ [(c), (d)] films with the doping concentration of 15 wt. %. (a) and (c) were taken under the excitation light of the spectral range of 330–385 nm with 420 nm barrier filter and (b) and (d) were taken under the excitation light of 460–490 nm with 520 nm barrier filter.

Downloaded 24 Mar 2008 to 68.181.190.164. Redistribution subject to AIP license or copyright; see http://jcp.aip.org/jcp/copyright.jsp

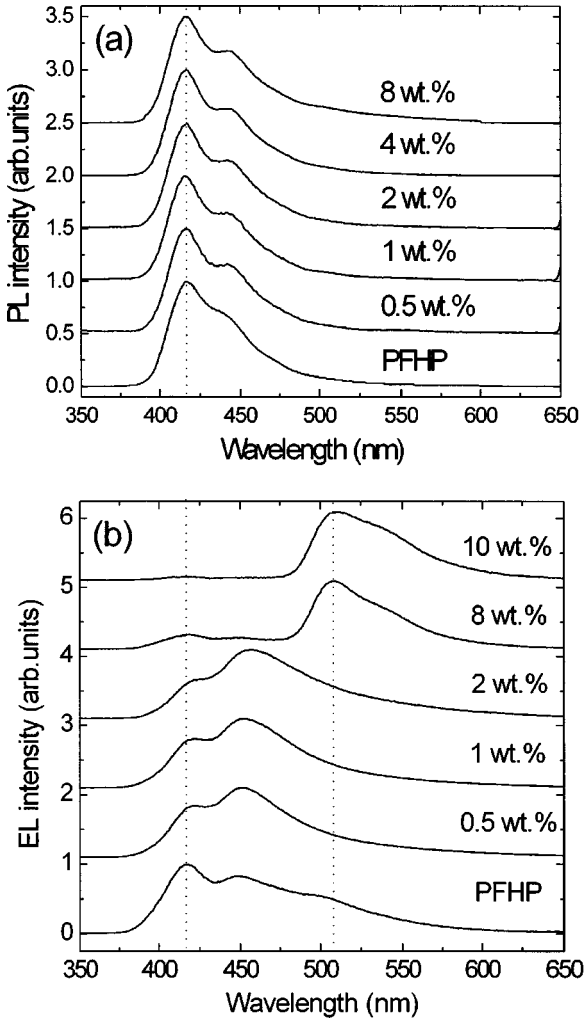

FIG. 13. (a) PL and (b) EL spectra of PFHP: $Ir(ppy)_3$ films with different doping concentrations (0, 0.5, 1, 2, 4, and 8 wt. %).

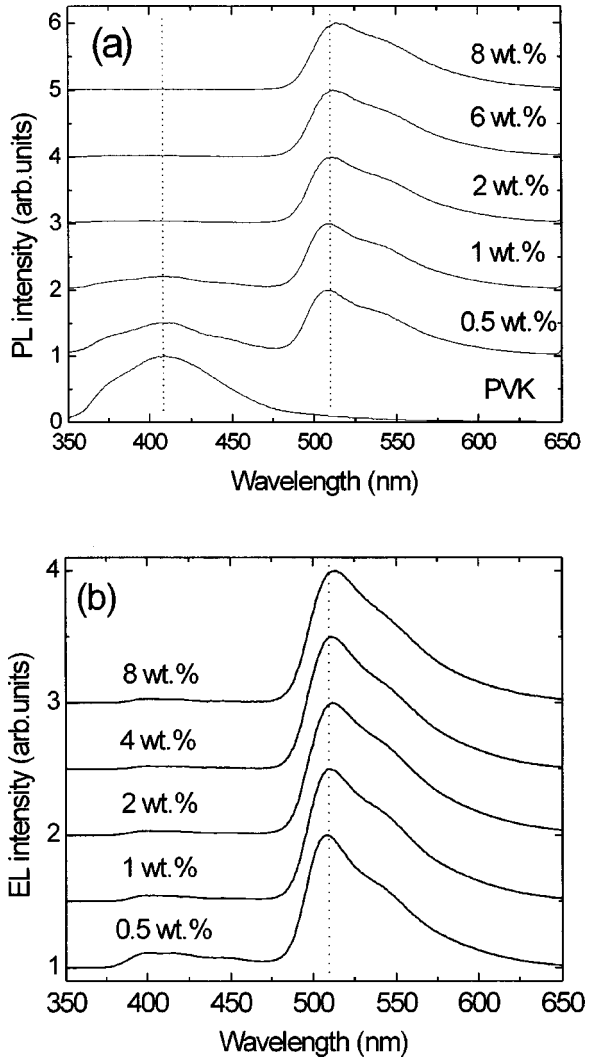

FIG. 14. (a) PL and (b) EL spectra of PVK: $Ir(ppy)_3$ films with different doping concentrations (0, 0.5, 1, 2, 6, and 8 wt. %).

eV, respectively, which were measured by ultraviolet photoelectron spectroscopy.

The PL and EL spectra of PVK:$Ir(ppy)_3$ show the green emission from $Ir(ppy)_3$ even at the low doping concentration of 1 wt. %, indicating that the singlet energy transfer is almost complete at the doping concentration (Fig. 14). The results are consistent with the homogeneous dispersion of the dopant with large Förster radius. Figure 15 shows the current density versus voltage characteristics of OLEDs with PFHP:$Ir(ppy)_3$ and PVK:$Ir(ppy)_3$ film as emissive layers. In the case of PFHP device, the turn-on voltage increased with increasing doping concentration as shown in Fig. 15(a). This result indicates the dopant molecules works as carrier traps in the device, which is consistent with the results of Fig. 13(b). Light emission from the recombination of the trapped charges on the dopant sites may be the major mechanism for PFHP:$Ir(ppy)_3$ devices. On the other hands, the PVK host devices show different behaviors from the PFHP host devices. The turn-on voltage increases with increasing doping concentration of $Ir(ppy)_3$ up to 1 wt. % but decreases when the doping concentration increased further to 8 wt. % as shown in Fig. 15(b). The results can be interpreted as follows. At low concentration, the dopant molecules behave as traps to increase the driving voltage. However, at high doping concentration, the dopants form another channel to transport carriers by hopping between the dopant molecules, thereby reducing the driving voltage. Thus, the various mechanisms (singlet, triplet energy transfer, and charge recombination on dopant site) may contribute to the emission process of PVK:$Ir(ppy)_3$ OLEDs.

Figure 16 shows the external quantum efficiencies (η_{ext}) of OLEDs using PVK:$Ir(ppy)_3$ and PFHP:$Ir(ppy)_3$ as the luminescent layers. The device with the emissive layer of PVK:$Ir(ppy)_3$ showed η_{ext} of 0.3% even at the low doping concentration of 0.1 wt. %. In contrast the η_{ext} of the $Ir(ppy)_3$:PFHP device was 0.1% and it was reduced as the current density increased. It is noteworthy that the light emitted from the $Ir(ppy)_3$:PFHP is mainly from PFHP not from $Ir(ppy)_3$ [Fig. 13(b)]. The difference in the quantum efficiency is even larger at the high doping concentration of 8 wt. %. The maximum external quantum efficiency of $\sim 6\%$ was obtained for PVK:$Ir(ppy)_3$ device at the current density of 7.4 mA/cm^2, which is 15 times higher value than that $\sim 0.4\%$ of PFHP:$Ir(ppy)_3$ at the current density of 0.8 mA/cm^2. These results clearly indicate that the formation

Downloaded 24 Mar 2008 to 68.181.190.164. Redistribution subject to AIP license or copyright; see http://jcp.aip.org/jcp/copyright.jsp

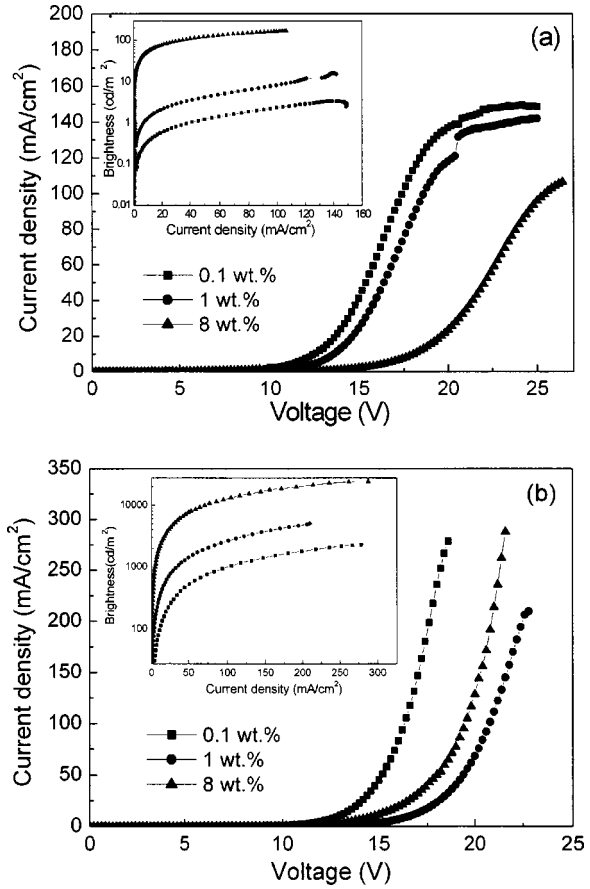

FIG. 15. Current density–voltage characteristics of $Ir(ppy)_3$ doped polymer LEDs with doping concentrations of 0.1 wt. % (filled squares), 1 wt. % (filled circles), and 8 wt. % (filled triangles) $Ir(ppy)_3$ in PFHP (a) and in PVK (b). Inset is the brightness–current density characteristics of the same devices.

of aggregates in the phosphorescent dye doped devices results in lower efficiency for the phosphorescent dye doped devices. Therefore, the homogeneous dispersion of a dopant in a host material must be addressed when doping systems for polymer LEDs are selected to utilize energy transfers to fabricate efficient devices.

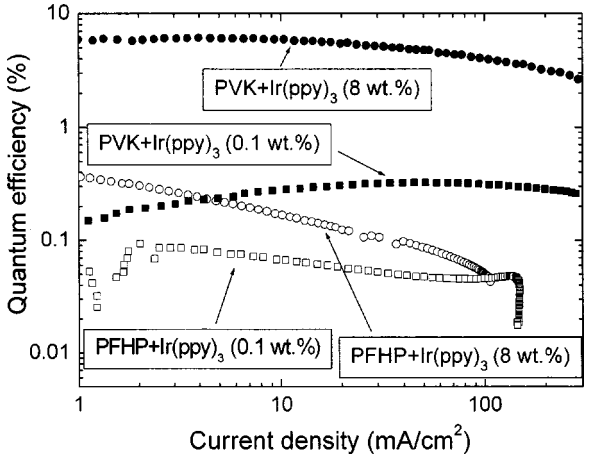

FIG. 16. The external quantum efficiency of $Ir(ppy)_3$ doped PVK and PFHP LEDs as a function of the current density.

VIII. CONCLUSIONS

Singlet and triplet–triplet energy transfer in phosphorescent dye doped polymer light emitting devices were investigated. Energy levels and dynamics of triplet-excited state in a π-conjugated polymer and a polymer with luminescent side chain chromophore were determined from low temperature luminescence studies. Singlet and triplet energy transfers are efficient in PVK doped with $Ir(ppy)_3$ or PtOEP as expected. They have (1) the large Förster radius, (2) high host T_1 energy level (2.46 eV), and (3) long lifetime of host T_1 state. However, the conditions do not represent the complete criteria for energy transfers for other systems as is evident from the absence of energy transfer from PFHP to the phosphorescent dyes. It was found that the absence of the energy transfers is originated from the formation of aggregates. The TEM, AFM, and fluorescence microscope images of $Ir(ppy)_3$ doped PFHP films showed the formation of aggregates, whereas PVK:$Ir(ppy)_3$ films showed homogeneous and smooth images. The formation of aggregates prevents dopant molecules from being in close proximity with host molecules thereby inhibiting energy transfer processes. It also explains the low efficiency from the PFHP:$Ir(ppy)_3$ LEDs. Therefore, homogeneous dispersion and chemical compatibility of dopant with host polymers along with the usual requirements of Förster and Dexter energy transfer must be considered in order to successfully prepare efficient phosphorescent dye doped polymer LEDs.

It is worthwhile to note that PVK, a polymer with emissive side chain chromophore, showed the large singlet–triplet splitting of 1.04 eV (8000 cm^{-1}) similar to π-conjugated polymers. It is not conclusive yet whether the large difference is a general character of the side chain polymers. However, we can conjecture at least, that the electron–electron interaction can be large because of the localized excited states in the polymer that leads to a large gap between S_1 and T_1 of PVK.[25,26] This result implies that it is difficult to find proper host polymers for efficient blue phosphorescent dyes from π-conjugated polymers or polymers with emissive side chain polymers, since the high T_1 state of the host is indispensable for efficient triplet–triplet energy transfer to blue phosphorescent dyes.

ACKNOWLEDGMENTS

The authors would like to thank Dr. Ho-Jun Song (KBSI, Kwang-Ju Branch) for low temperature PL experiment, Dr. R. R. Das, Ms. H. W. Lee (K-JIST), and Dr. Hyun-Nam Cho (KIST) for synthesizing $Ir(ppy)_3$ and PFHP, respectively. This work was financially supported by the NRL, BK21 program and the KOSEF through the Center for Electro- and Photo-Responsive Molecules in Korea University.

[1] M. A. Baldo, D. F. O'Brien, M. E. Thompson, and S. R. Forrest, Phys. Rev. B **60**, 14422 (1999).
[2] J. S. Wilson, A. S. Dhoot, A. J. A. B. Seeley, M. S. Khan, A. Kohler, and R. H. Friend, Nature (London) **413**, 828 (2001).
[3] Z. Shuai, D. Beljonne, R. J. Silbey, and J. L. Bredas, Phys. Rev. Lett. **84**, 131 (2000).
[4] M. Wohlgenannt, K. Tandon, S. Mazumar, S. Ramasesha, and Z. V. Vardeny, Nature (London) **409**, 494 (2001).

Downloaded 24 Mar 2008 to 68.181.190.164. Redistribution subject to AIP license or copyright; see http://jcp.aip.org/jcp/copyright.jsp

[5] R. H. Friend, R. W. Gymer, A. B. Holmes *et al.*, Nature (London) **397**, 121 (1999).
[6] M. A. Baldo, D. F. O'Brien, Y. You, A. Shoustikov, S. Sibley, M. E. Thompson, and S. R. Forrest, Nature (London) **395**, 151 (1998).
[7] M. A. Baldo, S. Lamansky, P. E. Burrows, M. E. Thompson, and S. R. Forrest, Appl. Phys. Lett. **75**, 4 (1999).
[8] M. Klessinger and J. Michl, *Excited States and Photochemistry of Organic Molecules* (VCH, New York, 1995).
[9] S. Capecchi, O. Renault, D.-G. Moon, M. Halim, M. Etchells, P. J. Dobson, O. V. Salata, and V. Christou, Adv. Mater. **12**, 1592 (2000).
[10] Z. Hong, C. Liang, R. Li, W. Li, D. Zhao, D. Fan, D. Wang, B. Chu, F. Zang, L.-S. Hong, and S.-T. Lee, Adv. Mater. **13**, 1241 (2001).
[11] C. Adachi, M. A. Baldo, and S. R. Forrest, J. Appl. Phys. **87**, 8049 (2000).
[12] C. Adachi, M. A. Baldo, S. R. Forrest, S. Lamansky, M. Thompson, and R. C. Kwong, Appl. Phys. Lett. **78**, 1622 (2001).
[13] C. Adachi, R. C. Kwong, P. Djurovich, V. Adamovich, M. A. Baldo, M. E. Thompson, and S. R. Forrest, Appl. Phys. Lett. **79**, 2082 (2001).
[14] C. Adachi, M. A. Baldo, and S. R. Forrest, Appl. Phys. Lett. **77**, 904 (2000).
[15] M. Ikai, S. Tokito, Y. Sakamoto, T. Suzuki, and Y. Taga, Appl. Phys. Lett. **79**, 156 (2001).
[16] T. Tsutsui, M.-J. Yang, M. Yahiro, K. Nakamura, T. Watanabe, T. Tsuji, Y. Fukuda, T. Wakimoto, and S. Miyaguchi, Jpn. J. Appl. Phys., Part 2 **38**, L1502 (1999).
[17] V. Cleave, G. Yahioglu, P. Le Barny, R. H. Friend, and N. Tessler, Adv. Mater. **11**, 285 (1999).
[18] M.-J. Yang and T. Tsutsui, Jpn. J. Appl. Phys., Part 2 **39**, L828 (2000).
[19] C.-L. Lee, K. B. Lee, and J.-J. Kim, Appl. Phys. Lett. **77**, 2280 (2000).
[20] P. A. Lane, L. C. Palilis, D. F. O'Brien, C. Giebeler, A. J. Cadby, D. G. Lidzey, A. J. Campbell, W. Blau, and D. D. C. Bradley, Phys. Rev. B **63**, 235206 (2001).
[21] N. Tessler, P. K. H. Ho, V. Cleave *et al.*, Thin Solid Films **363**, 64 (2000).
[22] V. Cleave, G. Yahioglu, P. Le Barny, D.-H. Hwang, A. B. Holmes, R. H. Friend, and N. Tessler, Adv. Mater. **13**, 44 (2001).
[23] S. Lamansky, R. C. Kwong, M. Nugent, P. I. Djurovich, and M. E. Thompson, Organic Electronics **2**, 53 (2001).
[24] M. A. Baldo and S. R. Forrest, Phys. Rev. B **62**, 10958 (2000).
[25] A. P. Monkman, H. D. Burrows, L. J. Hartwell, L. E. Horsburgh, I. Hamblett, and S. Navaratnam, Phys. Rev. Lett. **86**, 1358 (2001).
[26] Yu. V. Romanovskii, A. Gerhard, B. Schweitzer, U. Scherf, R. I. Personov, and H. Bässeler, Phys. Rev. Lett. **84**, 1027 (2000).
[27] K. A. King, P. J. Spellane, and R. J. Watts, J. Am. Chem. Soc. **107**, 1431 (1985).
[28] B. Xu and S. Holdcroft, J. Am. Chem. Soc. **115**, 8447 (1993).
[29] C. Hosokawa, H. Tokailin, H. Higashi, and T. Kusumoto, Appl. Phys. Lett. **60**, 1220 (1992).
[30] V. Savvateev, A. Yakimov, and D. Davidov, Adv. Mater. **11**, 519 (1999).
[31] C. Rothe and A. P. Monkman, Phys. Rev. B **65**, 075104 (2002).
[32] C. Rothe, S. Hintschich, A. P. Monkman, M. Svensson, and M. R. Anderson, J. Chem. Phys. **116**, 10503 (2002).
[33] D. L. Dexter, J. Chem. Phys. **21**, 836 (1953).
[34] T. Forster, Discuss. Faraday Soc. **27**, 7 (1959).
[35] A. A. Shoustikov, Y. You, and M. E. Thompson, IEEE J. Sel. Top. Quantum Electron. **4**, 3 (1998).
[36] R. Stevenson, R. Riehn, R. G. Milner, D. Richards, E. Moons, D.-J. Kangs, M. Blamire, J. Morgado, and F. Cacialli, Appl. Phys. Lett. **79**, 833 (2001).
[37] L. M. Herz, C. Silva, R. H. Friend, and R. T. Phillips, Phys. Rev. B **64**, 195203 (2001).

Downloaded 24 Mar 2008 to 68.181.190.164. Redistribution subject to AIP license or copyright; see http://jcp.aip.org/jcp/copyright.jsp